

# Direct reconstruction of the pp – elastic scattering amplitudes at U70

A A Bogdanov<sup>1</sup>, VA Chetvertkova<sup>4</sup>, A V Kozelov<sup>2</sup>, V P Ladygin<sup>3</sup>, V Mochalov<sup>1,2</sup>,  
M B Nurusheva<sup>1</sup>, V A Okorokov<sup>1</sup>, M F Runtso<sup>1</sup> and A N Vasiliev<sup>1,2</sup>

<sup>1</sup> National Research Nuclear University (Moscow Engineering Physics Institute), Moscow, 115409, Russia

<sup>2</sup> NRC «Kurchatov Institute» - IHEP, Protvino, Moscow region, 142281, Russia

<sup>3</sup> Joint Institute for Nuclear Research, Dubna, Moscow region, 141980, Russia

<sup>4</sup> GSI, Plankstrasse 1, 64291, Darmstadt, Germany

E-mail: [mbnurusheva@mail.ru](mailto:mbnurusheva@mail.ru)

**Abstract.** The direct reconstruction of pp elastic scattering amplitudes at the SPASCHARM experiment is discussed. The observables are expressed in terms of invariant amplitudes. These amplitudes are deduced analytically by solving bilinear relations.

Monte-Carlo simulations of elastic scattering as well background reactions were carried out. Elastic and diffraction interactions of protons were simulated by using PYTHIA generator for 16 GeV incident protons, designed Setup geometry and the resolution of the detectors. The criteria to select elastic processes are discussed and presented. Two-dimensional distributions of the product of the tangents of the polar angles of the recoil particle and the scattered particle versus difference of the azimuth angles of these particles, were obtained. The estimated ratio of the signal to background  $S/(S+B)$  is about 0.99.

## 1. Introduction

Newly developing experiment SPASCHARM (SPin ASymmetry in CHARMonia) at U-70 accelerator will give the unique possibility to measure spin effects with the use of polarized proton and antiproton beams and polarized targets. The SPASCHARM experiment also requires development of the polarimetry [1] to verify beam polarization, which will help to study spin effects in elastic processes, since the detectors are the same in both cases.

The concept of the scattering matrix presented by theorists is convenient for describing of the elastic reactions, but the matrix elements cannot be measured directly. Therefore, it is necessary to determine a set of observables, which allows the direct reconstruction of the scattering matrix. Direct Reconstruction of the spin amplitudes (DRSA) is a fully model-independent analysis using only fundamental conservation laws.

The first DRSA analysis was carried out using the 0.429 GeV at the Chicago University (1968) [2]. Before 1975, the direct reconstruction for pp elastic scattering was only done at  $90^\circ$  (c.m.s.) at a few energies [3]. The first direct reconstruction at a large angular region was carried out in PSI and was reported in 1981 [4] for the 0.59 GeV and in 1990 for the data below 0.59 GeV [5]. Similar reconstructions have been subsequently performed using LAMPF data at 0.73 GeV [6] and at 0.80 GeV. The SATURNE II data have also allowed a DRSA analysis at 11 energies between 0.83 and



2.70 GeV [8]. Finally, at higher energy, an amplitude analysis was performed using the 6 GeV/c ANL-ZGS data [9,10]. Up to now, direct reconstruction of amplitudes for pp-elastic scattering has been performed only for the energies below 6 GeV/c, while there is no any data available for p(bar)p - elastic scattering.

## 2. Formalism and observables

Assuming parity conservation, time reversal and isospin invariance, the scattering matrix is written in terms of complex amplitudes a, b, c, d and e [11]

$$M(\mathbf{k}_f, \mathbf{k}_i) = \frac{1}{2} \{ (a + b) + (a - b) (\boldsymbol{\sigma}_1, \mathbf{n}) (\boldsymbol{\sigma}_2, \mathbf{n}) + (c + d) (\boldsymbol{\sigma}_1, \mathbf{m}) (\boldsymbol{\sigma}_2, \mathbf{m}) + (c - d) (\boldsymbol{\sigma}_1, \mathbf{l}) (\boldsymbol{\sigma}_2, \mathbf{l}) + e (\boldsymbol{\sigma}_1 + \boldsymbol{\sigma}_2, \mathbf{n}) \}, \quad (1)$$

$$\mathbf{l} = \frac{\mathbf{k}_f + \mathbf{k}_i}{|\mathbf{k}_f + \mathbf{k}_i|}, \quad \mathbf{m} = \frac{\mathbf{k}_f - \mathbf{k}_i}{|\mathbf{k}_f - \mathbf{k}_i|}, \quad \mathbf{n} = \frac{\mathbf{k}_f \times \mathbf{k}_i}{|\mathbf{k}_f \times \mathbf{k}_i|}, \quad (2)$$

where  $k_i$  and  $k_f$  are unit vectors in the direction of the incident and scattered particle momenta in the c.m.s. The spin matrices  $\boldsymbol{\sigma}_1$  and  $\boldsymbol{\sigma}_2$  (the Pauli matrices) act on the first and the second nucleon wave functions, respectively.

Let introduce some notation. We denote a general scattering observables as  $X_{srbt}$ , where the indices denote the spin direction of the particles: s - scattered, r - recoil, b - beam, t - target, and  $X_{srbt} = \sigma X_{srbt}$  is cross-section times observables.

There is a possibility to have polarized proton beam oriented in all three directions and the target polarized vertically and longitudinally. Therefore, the SPASCHARM configuration allow us to measure following non-vanishing observables:  $A_{oono}$  - beam analyzing power,  $A_{oono}$  - target analyzing power,  $A_{oonm}$ ,  $A_{oolb}$ ,  $A_{ooml}$  - spin correlations. Also polarization of the recoil proton can be measures with the use of the large aperture polarimeter:  $P_{onoo} = A_{onoo} = A_{oono}$  - the polarization of the recoil proton  $P_{onoo}$  is the same as analyzing power. Also following observables can be measured: three polarization transfer coefficients from the beam to the recoil particle ( $K_{onno}$ ,  $K_{ommo}$ ,  $K_{omlo}$ ), two depolarization coefficients for the target ( $D_{onon}$ ,  $D_{omol}$ ), five polarizations of the recoil particle ( $N_{onll}$ ,  $N_{onml}$ ,  $N_{omnl}$ ,  $N_{omln}$ ,  $N_{ommn}$ ). Therefore, 15 diferent observables in total can be measured at U70.

The measured observables in terms of scattering amplitudes are expressed as follows:

$$\begin{aligned} \sigma &= \frac{1}{2} [ |a|^2 + |b|^2 + |c|^2 + |d|^2 + |e|^2 ] \\ \sigma A_{oonn} &= \frac{1}{2} [ |a|^2 - |b|^2 - |c|^2 + |d|^2 + |e|^2 ] \\ \sigma K_{onno} &= \frac{1}{2} [ |a|^2 - |b|^2 + |c|^2 - |d|^2 + |e|^2 ] \\ \sigma D_{onon} &= \frac{1}{2} [ |a|^2 + |b|^2 - |c|^2 - |d|^2 + |e|^2 ] \end{aligned} \quad (3)$$

Measurement or the cross section of  $A_{oonn}$ ,  $K_{onno}$  and  $D_{onon}$ , allows to reconstruct the following amplitudes or their combinations:

$$\begin{aligned} |b|^2 &= \frac{\sigma}{2} [ 1 - A_{oonn} - K_{onno} + D_{onon} ] \\ |c|^2 &= \frac{\sigma}{2} [ 1 - A_{oonn} + K_{onno} - D_{onon} ] \\ |d|^2 &= \frac{\sigma}{2} [ 1 + A_{oonn} - K_{onno} - D_{onon} ] \\ |a|^2 + |e|^2 &= \frac{\sigma}{2} [ 1 + A_{oonn} + K_{onno} + D_{onon} ] \end{aligned} \quad (4)$$

The analyzing powers (or polarization of recoil particle) equal  $\sigma A_{oono} = \sigma A_{oono} = \sigma P_{onoo} = Re \bar{a} e$ . Taking into account that  $X_{srbt} = \sigma X_{srbt}$ , the required expressions are following:  $A_{ooml} = -Im \bar{d} e$ ,  $A_{ooll} = -Re(\bar{a} d - \bar{b} c)$ ,  $D_{omol} = -Im \bar{b} e$ ,  $K_{omlo} = -Im \bar{c} e$ ,  $K_{ommo} = Re(\bar{a} c + \bar{b} d)$ ,  $N_{ommn} = Re \bar{c} e$ ,  $N_{onll} = -Re \bar{d} e$ ,  $N_{omln} = Im(\bar{a} c - \bar{b} d)$ ,  $N_{omnl} = Im(\bar{a} b - \bar{c} d)$ ,  $N_{onml} = Im(\bar{a} d + \bar{b} c)$ .

At first we chose the amplitude  $d$  to be real and positive and introduced notations for the real and imaginary parts for each amplitudes  $Re d = d_1$ ,  $Im d = 0$ ,  $a = a_1 + ia_2$ ,  $b = b_1 + ib_2$ ,  $c = c_1 + ic_2$ ,  $e = e_1 + ie_2$ . Following expressions were obtained for all amplitudes:

$$\begin{aligned}
 c_1 &= \frac{d_1 (Aooml Komlo - Nommn Nonll)}{Aooml^2 + Nonll^2} \quad c_2 = -\frac{d_1 (Aooml Nommn + Komlo Nonll)}{Aooml^2 + Nonll^2} \quad e_1 = -\frac{Nonll}{d_1} \quad e_2 = -\frac{Aooml}{d_1} \\
 a_1 &= \frac{-Aooml Domol d_1^2 - Aoono Nommn d_1^2 + Aooml^2 Kommo - Aooml Nomln Nonll}{d_1 (Aooml Komlo + Nommn Nonll)} \\
 a_2 &= -\frac{Aoono Komlo d_1^2 - Domol Nonll d_1^2 + Aooml Kommo Nonll - Nomln Nonll^2}{d_1 (Aooml Komlo + Nommn Nonll)}, \\
 b_1 &= \left( Aooml^2 Domol Komlo d_1^2 - Aoono Komlo^2 Nonll d_1^2 - Aoono Nommn^2 Nonll d_1^2 \right. \\
 &\quad \left. + Domol Komlo Nonll^2 d_1^2 + Aooml^2 Komlo Nomln Nonll + Aooml^2 Kommo Nommn Nonll \right. \\
 &\quad \left. + Komlo Nomln Nonll^3 + Kommo Nommn Nonll^3 \right) / \left( d_1 (Aooml^2 + Nonll^2) (Aooml Komlo + Nommn Nonll) \right) \\
 b_2 &= \left( -Aooml^2 Domol Nommn d_1^2 - Aooml Aoono Komlo^2 d_1^2 - Aooml Aoono Nommn^2 d_1^2 \right. \\
 &\quad \left. - Domol Nommn Nonll^2 d_1^2 + Aooml^3 Komlo Nomln + Aooml^3 Kommo Nommn \right. \\
 &\quad \left. + Aooml Komlo Nomln Nonll^2 + Aooml Kommo Nommn Nonll^2 \right) / \left( d_1 (Aooml^2 + Nonll^2) (Aooml Komlo + Nommn Nonll) \right) \\
 d_1 &= \left( (Aooml^2 + Komlo^2 + Nommn^2 + Nonll^2) (Aoono Komlo - Domol Nonll) (Aooml^2 + Nonll^2) \right. \\
 &\quad \left. (Aooml Komlo Nonml - Aooml Kommo Nonll + Komlo^2 Nomln + Komlo Kommo Nommn + Nomln Nonll^2 + Nommn Nonll Nonml) \right)^{1/2} / \left( (Aooml^2 + Komlo^2 + Nommn^2 + Nonll^2) (Aoono Komlo - Domol Nonll) \right)
 \end{aligned} \tag{5}$$

Since the expressions obtained are rather complex, we decided also to perform calculations if amplitude  $e$  is real and positive, and got following equations for amplitudes:

$$\begin{aligned}
 a_2 &= -\frac{1}{(Aooml Komlo + Nommn Nonll) e_1} \left( -Aooml Kommo e_1^2 + Nomln Nonll e_1^2 + Aooml^2 Domol + Aooml Aoono Nommn - Aoono Komlo Nonll + Domol Nonll^2 \right), \\
 b_1 &= \frac{1}{e_1 (Aooml Komlo + Nommn Nonll)} \left( -Komlo Nomln e_1^2 - Kommo Nommn e_1^2 + Aooml Domol Nommn + Aoono Komlo^2 + Aoono Nommn^2 - Domol Komlo Nonll \right), \\
 a_1 &= \frac{Aoono}{e_1} \quad b_2 = \frac{Domol}{e_1} \quad c_1 = \frac{Nommn}{e_1} \quad c_2 = \frac{Komlo}{e_1} \quad d_1 = -\frac{Nonll}{e_1} \quad d_2 = \frac{Aooml}{e_1} \\
 e_1 &= \left( (Aooml Komlo Nonml - Aooml Kommo Nonll + Komlo^2 Nomln + Komlo Kommo Nommn + Nomln Nonll^2 + Nommn Nonll Nonml) (Aooml^2 + Komlo^2 + Nommn^2 + Nonll^2) (Aoono Komlo - Domol Nonll) \right)^{1/2} / \left( (Aooml Komlo Nonml - Aooml Kommo Nonll + Komlo^2 Nomln + Komlo Kommo Nommn + Nomln Nonll^2 + Nommn Nonll Nonml) \right)
 \end{aligned} \tag{6}$$

The equations for amplitudes are more compact and convenient when we choose the amplitude  $e$  to be real and positive. The minimal set of observables for direct reconstruction of the scattering amplitudes consists of cross section  $\sigma$  and nine spin observables:  $A_{oono}$ ,  $A_{ooml}$ ,  $K_{omlo}$ ,  $K_{ommo}$ ,  $D_{omol}$ ,  $N_{omln}$ ,  $N_{onml}$ ,  $N_{ommn}$ ,  $N_{onll}$ .

### 3. Monte Carlo simulation of elastic reactions

The use of elastic processes to determine the absolute value of polarization makes it possible to measure the polarization of protons and (anti) protons for any particle energy. Nevertheless the optimal energy to obtain antiproton beam is 16 GeV due to high pion background [12]. At lower energies, the number of background particles in the beam sharply increases, and with beam energy increase, the cross section decreases. Therefore, it is proposed to carry out the measurements precisely at 16 GeV, and simulation was performed for this energy. The beam tagging system allows to measure polarization and momentum for each beam particle with an accuracy better than 1%, as well as the coordinates and angles of the particles on the target. One can choose elastic events by complanarity and matching the scattering angles and the particle momentum.

$10^6$  events were simulated using the PYTHIA 6.3 generator to estimate background contamination from diffraction processes, in which two charged particles enter the detector. Real geometry and resolution of the detector were taken into account in the simulation as well as beam properties.

#### 3.1 Estimating the size of the detector

The detector scheme and sizes are presented on figure 1 and table 1.

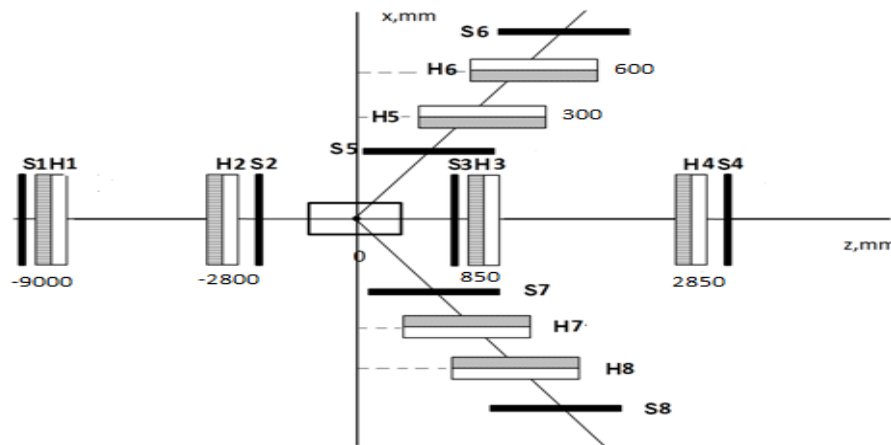


**Figure 1.** Scheme of the detector for measuring the elastic processes.

The detector dimensions have been selected [13], based on the beam characteristics [12]. The scintillators of the hodoscopes are located “comb”, and although the width of each scintillator is 6 mm, this arrangement allows us to know the coordinate of the particle’s impact with a step of 2 mm. The detector in paper [13] was designed for 45 GeV beam. Here detector sizes were changed to carry out the measurements both at 16 and 45 GeV.

**Table 1.** The sizes of the recoil and scattering detector components, designed for 16 GeV/c.

Hodoscope	Distance from target ( mm)	Total dimension (mm)	Dimension of scintillator strips: Width×Thickness×Length (mm <sup>3</sup> )		Numbers of channels	
			X	Y	X	Y
Forward Hodoscopes						
H3	850	84 × 84	6 × 3 × 84	6 × 3 × 84	18	18
H4	2850	182 × 86	6 × 3 × 182	6 × 3 × 86	45	21
Recoil Hodoscopes						
	X	Z × Y	Z	Y	Z	Y
H5 - H7	300	322 × 228	9 × 5 × 322	9 × 5 × 228	51	37
H6 - H8	600	432 × 430	9 × 5 × 432	9 × 5 × 420	71	69

Since the angles are the same for both momenta, the sizes of the recoil hodoscopes (H5 and H7) will be the same. The distribution of the scattered particles for 16 GeV turned out to be wider, therefore the dimensions of the forward hodoscope (H3) were increased. Simulated coordinate distributions of the scattered and recoiled protons on the hodoscope planes are presented on figure 2 and figure 3 correspondingly only for elastic events, when both particles hit detectors.

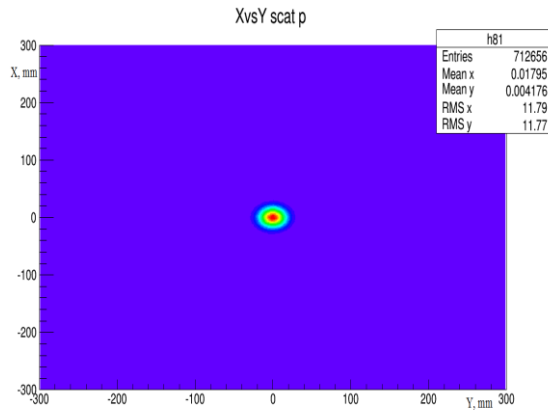


**Figure 2.** Distribution of scattered protons in the XY plane, where the scattered proton hodoscope is located

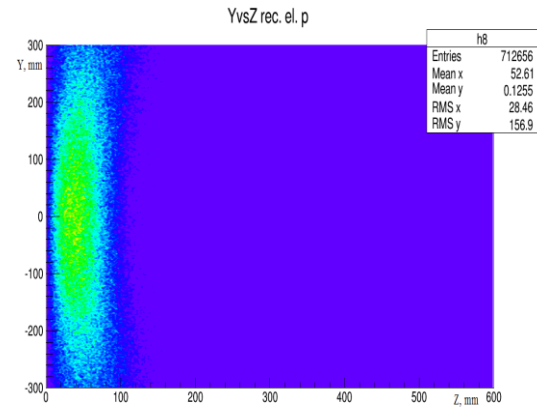


**Figure 3.** Distribution of recoil protons in the YZ plane, where the recoil proton hodoscope is located

Two-dimensional histograms (figures 4 and 5) show the dependence of the tangent products of scattered and recoil protons on the difference of its azimuthal angles for elastic and diffraction processes correspondingly, taking into account the dimensions of the detectors H3 and H5.

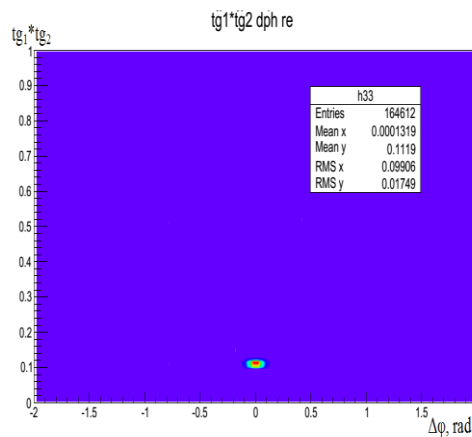


**Figure 4.** The dependence of the products of tangents of recoil and scattered particles on the difference of its azimuthal angles only for elastic processes

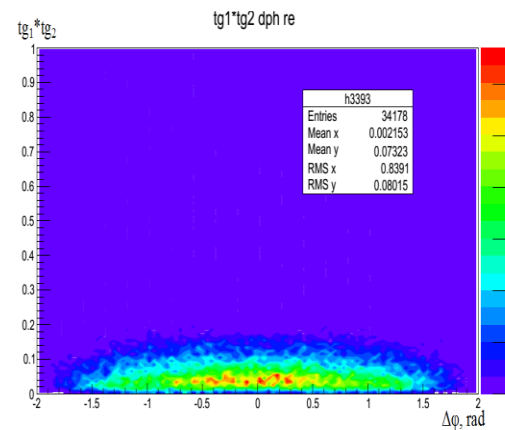


**Figure 5.** The same dependence but for diffraction processes

Using the information from two-dimensional distributions (figure 4), it is possible to choose following range in which elastic processes should be measured:  $-0.2 < \Delta\phi < 0.2$  and  $0.09 < tg1 \cdot tg2 < 0.14$ . The plots on figure 6 show, that the use of intervals of  $\Delta\phi$  and  $tg1 \cdot tg2$  selected significantly suppress background diffraction events with a slight suppression of the signal. The ratio of the signal to background  $S/(S + B)$  is 0.995

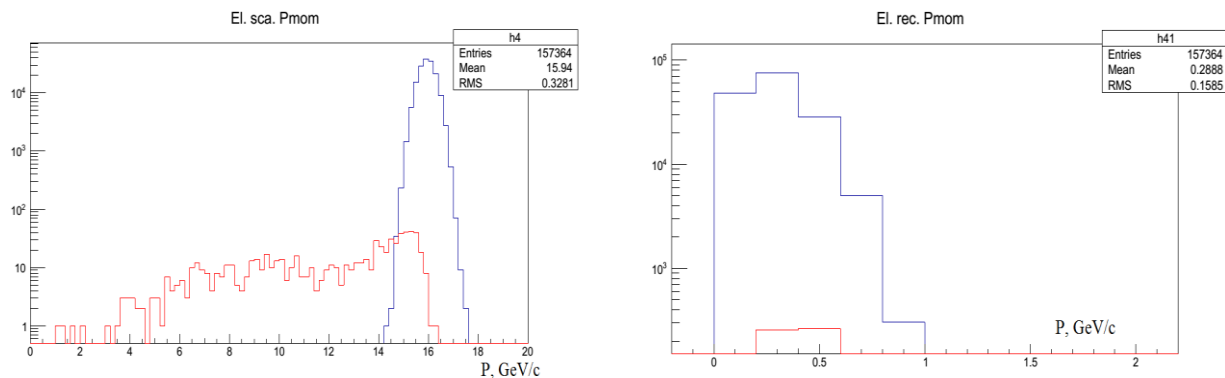


**Figure 6.** The momentum distributions of the scattered (left) and recoil (right) particles. Blue line is elastic processes, red line – the diffraction processes.

#### 4. Summary

The proposal for a direct reconstruction of the amplitudes of pp elastic scattering in the SPASCHARM experiment is presented. The observables are expressed through invariant amplitudes. These amplitudes are derived analytically. A minimal set of spin observables was determined. It turned out that to restore all nine elements of the matrix (5 complex amplitudes, one of which is fixed as real), it is enough to measure the cross section and nine spin observables. Monte Carlo simulations for real sizes and resolution of detectors showed that the calculated signal-to-background ratio  $S/(S+B)$  is about 0.99 for the selected criteria.

The work has been supported in part by the NRNU MEPHI Academic Excellence Project (contract № 02.a 03.21.0005, 27.08.2013) and by RFBR, project number 18-02-00006.

#### References

- [1] Bogdanov A A *et al* 2016 *J. Phys.: Conf. Ser.* **678** 012034
- [2] Lemon P *et al* 1968 *Phys. Rev.* **169** 1026
- [3] Lechanoine-Leluc C and Lehar F 1993 *Rev. Mod. Phys.* **65** 47
- [4] Aprile J E *et al* 1981 *Phys. Rev. Lett.* **46** 1047
- [5] McNaughton M W *et al* 1990 *Phys. Rev. C* **41** 2809
- [6] Hausammann J R *et al* 1989 *Phys. Rev. D* **40** 22
- [7] Arash F *et al* 1985 *Phys. Rev. D* **32** 74
- [8] Lac C D *et al* 1990 *Journal de Physique*, 1990, **51** 2689-2716
- [9] Matsuda M, Suemitsu H, Yonezawa M 1986 *Phys. Rev. D* **33** 2563
- [10] Auer P *et al* 1985 *Phys. Rev.* **032** 1609
- [11] Bystricky J, Lehar F and Winternitz P 1978 *Journal de Physique* **39** 1-32
- [12] Abramov V V *et al* 2018 *Nuclear Instr. and Methods in Physics Research A* **901** 62–68
- [13] Abramov V V *et al* 2017 *J. Phys.: Conf. Ser.* **938** 012006